JOURNAL OF MATERIALS SCIENCE **36** (2001) 2499–2504

# Kinetic study on the surface oxidation of the molten Mg-9Al-0.5Zn-0.3Be alloy

X. Q. ZENG, Q. D. WANG, Y. Z. LU, W. J. DING, C. LU,
Y. P. ZHU, C. Q. ZHAI, X. P. XU
*Shanghai Jiao Tong University, Shanghai, 200030, People's Republic of China*
*E-mail: zxq70810@mail1.sjtu.edu.cn*

Be addition make the oxide film formed on the molten magnesium alloy denser and tougher, thus the burning of the Mg during melting was suppressed. AES was employed to study the composition of the oxide film growing on the surface of the molten Mg-9Al-0.5Zn-0.3Be alloy. It was suggested that the surface oxide film could be divided to two layers: the outer MgO layer and the inner mixed layer consisting of MgO and BeO. Both experimental results and theory analysis indicated that the outer layer grew under parabolic law and the thickness almost kept unchanged during the steady growing state for the inner layer. 

## 1. Introduction

The applications of magnesium alloy are expanding with a high speed thanks to their low density and many other advantages [1–4], but the burning of magnesium during melting makes the magnesium parts hard to be produced. In order to solve this problem, fluxes or protective gases have to be used as oxidation inhibitator [5–8]. However, atmospheric pollution and some other disadvantages were brought by the above two methods, so investigators hope to suppress the ignition of Mg during melting by means of another method—alloying, which has little harm to the environment.

It was proved that some elements such as Al, Ca and Be could increase the oxidation resistance of Mg [9–13]. Generally, small quantity of Be was added to the most common used diecasting AZ91 magnesium alloy [14]. Keith reported even as small quantities as 5 to 100 ppm of Be addition could dramatically reduced the oxidation of magnesium [15]. However, both the structure of the oxide film and the oxidation process on the surface of the molten Be-bearing magnesium alloy are not clear.

In the present study, the structure of the oxide film on the surface of molten Be-containing magnesium alloy and the oxidation kinetic analysis was studied. Furthermore, a simplified model was established to describe the oxidation process on the surface of the molten Mg-9Al-0.5Zn-0.3Be alloy.

## 2. Experimentals

The Mg-9Al-0.5Zn-0.3Be alloy was melt with electric resistance furnace and ingots with the size of $\phi$ $80 \times 50$ mm were obtained. The oxide film samples shown in Table I were prepared with following process. The ingot was remelt in a 100 mm-diameter iron crucible that was placed in the furnace. When the temperature reached the previously selected value, the original oxides on the surface of the molten alloy were removed with a steel spatula to obtain the refresh surface. For sample No. 2 to No. 5, which were oxidized at 650°C for various time, the crucibles were removed from the furnace carefully as soon as the previously selected oxidation time was reached and cooled in the air. For sample No. 1 and sample No. 6 to No. 9, they were oxidized at various temperatures. When the previously selected temperatures were reached, the molten alloys on crucibles were then taken out and poured onto a steel plate; thus, these samples have the same long oxidation time.

The concentration of beryllium was analyzed with Inductively Coupled Plasma spectrum machine (Plasma 400) produced by Perkin Elmer Company. The real concentration of beryllium is about 0.1% in the studied alloy, which means the recovery rate of beryllium is 30% or so.

The specimens with the size of $4 \times 4 \times 2$ mm were cut from the oxide film samples and cleaned with acetone. The elemental composition and the depth-profile in the surface oxide film were estimated using Auger electron spectroscopy (AES) in conjunction with argon-ion sputtering. A PHI550ESCA/SAM apparatus with standard pressure of $1 \times 10^{-9}$ Torr in the chamber and cylindrical mirror analyzer were used for AES measurements. The argon-ion bean voltage and current were 3 KeV and 100 $\mu$A/cm$^2$ respectively.

## 3. Results

Fig. 1 shows the typical Auger pattern obtained on the surface of the specimen No. 1 after 1 minute $Ar^+$ sputtering. The low energy peaks of magnesium and aluminum are sensitive to the surface contamination, so the high energy peaks were used during quantification performance. The calculation formula of the elemental

TABLE I Oxidation parameters of the samples

| NO. | Oxidation time (s) | Temperature (°C) |
|---|---|---|
| 1 | 10 | 650 |
| 2 | 600 | 650 |
| 3 | 900 | 650 |
| 4 | 1800 | 650 |
| 5 | 3600 | 650 |
| 6 | 10 | 620 |
| 7 | 10 | 680 |
| 8 | 10 | 710 |
| 9 | 10 | 740 |


*Figure 1* Typical Auger Spectra investigated on the surface of the Mg-9Al-0.5Zn-0.3Be alloy specimen.

concentration is [16]:

$$C_{\mathrm{x}} = \frac{I_{\mathrm{x}}}{S_{\mathrm{x}}} \Big/ \sum \frac{I_{\mathrm{a}}}{S_{\mathrm{a}}} \tag{1}$$

where $I_{\mathrm{x}}$ ans $S_{\mathrm{x}}$ denote the peak-to-peak height and the sensitive factor of the element X respectively.

Fig. 2 shows the depth profiles from specimen No. 1 to No. 5 as the function of the sputtering time. It can be seen, the oxide film growing on the surface of the molten Mg-9Al-0.5Zn-0.3Be alloy can be divided to two layers: outer layer and inner layer, which are marked by dash lines. The outer layer, whose range is from the air/oxide interface to the position where the oxygen concentration begins to decrease greatly, mainly consists of Mg and O. Within this layer, the concentrations of Mg and O almost keep constant and the concentration ratio of Mg/O is a little greater than 1, indicating that the $Mg^{2+}$ is excess. This result is coincident with the opinion that MgO is *n*-type semiconductor, in which metallic cations are excess.

The inner layer is from the downside interface of the outer layer to the position where the oxygen concentration decreases to the half value of the outer layer. In this layer, magnesium concentration decreases greatly at first and then increases greatly, just like the alphabet "V". This V-shape distribution of magnesium can be explained as follows. With the depth decreasing, the concentration of oxidized Mg decreases, whereas the concentration of metallic Mg increases gradually. Thus, the overlap of the metallic magnesium and the oxidized magnesium results in the V-shape distribution of magnesium in the inner layer. For Be, its concentration increases sharply from the outer/inner layer interface and decreases after reaching a maximum value and just like an inversed "V". The aluminum concentration increases slowly in the inner layer. Based on these observations, the inner layer is considered to be a mixed layer of MgO and BeO. Under the oxide film, the concentrations of all elements are close to their original concentrations gradually.

According to the above rules, the thickness of outer layer and inner layer on all specimens were obtained and shown as the function of oxidation time in Fig. 3. It should be noted that the mean sputtering rate of argon-ion on the studied film is hard to be obtained, so $L = R \times t$ is regarded as the thickness where $R$ (nm/min) represents the mean sputtering rate and $t$ (min) is the sputtering time. As shown in Fig. 3a, the growing rate of the outer layer is high at first and declines later. Thus, we suppose that the outer layer might grow under parabolic law. Fig. 3c shows the square of the outer layer thickness ($L^2$) as the function of the oxidation time. It is suggested that $L^2$ is approximately proportional to the oxidation time, indicating that the outer layer grows under parabolic law. For the inner layer, it is shown in Fig. 3b that its thickness increases with the time at a fairly slow rate and we could even consider that it keeps unchanged in the long time.

Fig. 4 shows the depth profiles of specimen No. 6 to 9, which were oxidized at various temperatures for same long time. Except the thickness, the distributions of all elements are similar to the previous figures. In the same way, the thickness of the outer layers is obtained and shown as the function of temperature in Fig. 5a. This curve is supposed to be an exponential curve, so the $\ln L \sim 1/T$ curve was plotted in Fig. 5b. Obviously, $\ln L$ is linear to $1/T$ approximately, suggesting that the thickness of the outer layer increases exponentially with the oxidation temperature.

## 4. Discussion

Both MgO and BeO are n-type oxide according to the semiconductor chemistry theory [17]. As shown in Fig. 6, the metallic cations are excess and exist as interstitial ions in MgO. During high temperature oxidation, one Mg atom is ionized to one $Mg^{2+}$ and two electrons at the metal/oxide interface, Then, both cations and electrons enter the oxide and become interstitial cations $Mg^{2+}$ and interstitial electrons $e^-$. Under the drive of the electric potential gradient and chemical potential gradient, both $Mg^{2+}$ and $e^-$ move to the air/oxide interface and react with the absorbed oxygen to form MgO.

Fig. 7 shows the model that was established to describe the oxidation process on the surface of the molten Mg-9Al-0.5Zn-0.3Be alloy. First of all, some hypothesis should be emphasized:

(I) Only Mg and Be are oxidized
(II) MgO and BeO don't dissolve each other
(III) The oxide grows via the outerward diffusion of metallic cations

Three stages are believed to be experienced during the oxidation of the metal; they are absorption stage, rapid growing stage and steady growing stage.

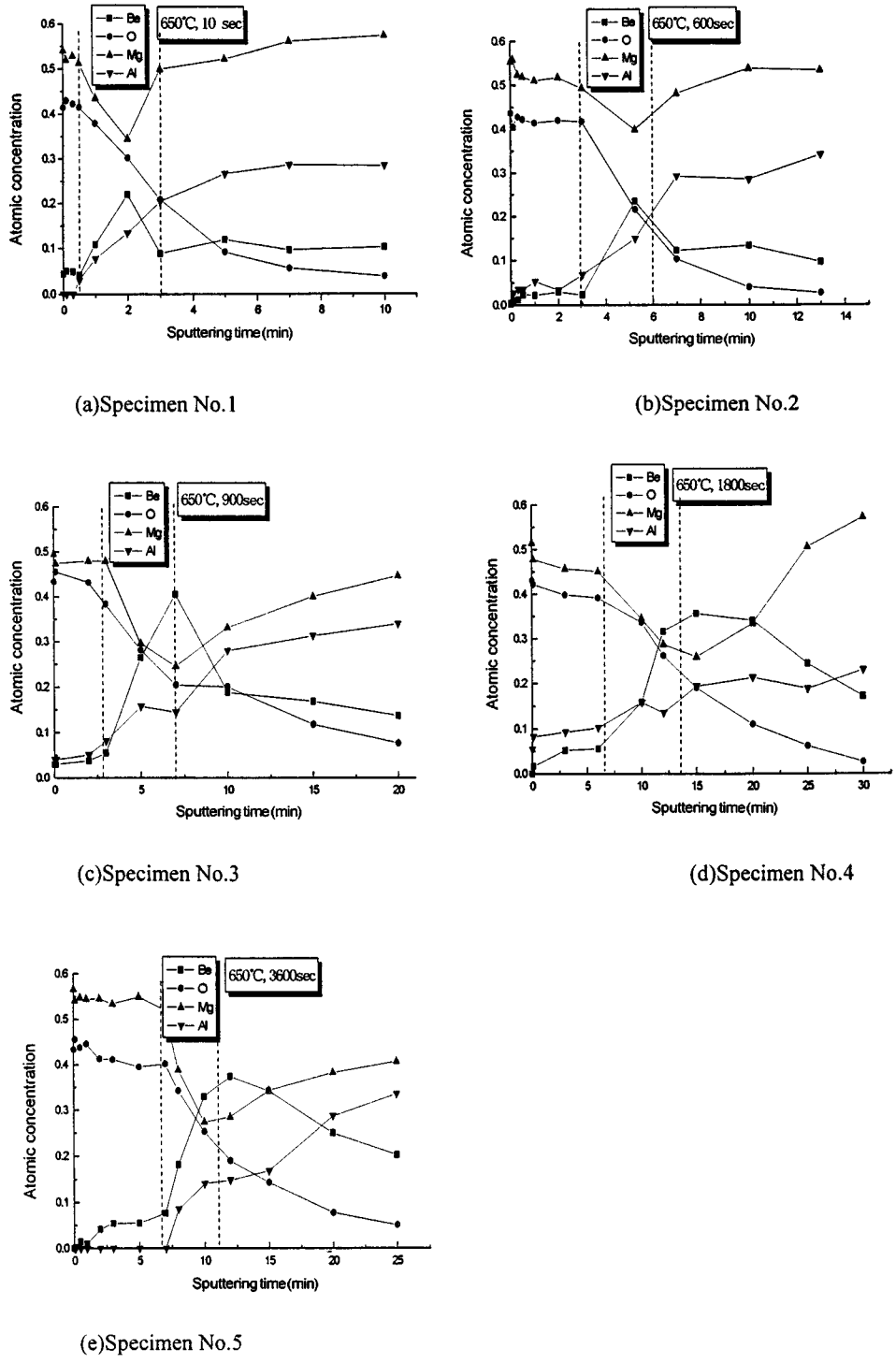


*Figure 2* Depth profiles on the surface oxides of specimen No. 1 to No. 6.

During the absorption stage, the oxygen molecules, which impact on the surface of the molten alloy with high frequency, are absorbed on the surface and decomposed into two atoms. The Mg concentration in the alloy is so high that it will react with the absorbed oxygen prior to Be. So a thin MgO film will cover on the surface of the molten alloy within short time.
The reactions happen in this stage are:

$$O_2 = 2O \tag{2}$$

$$Mg^{2+} + 2e^- + O = MgO \tag{3}$$

As soon as the thin MgO film covers on the surface of the molten alloy completely, the oxidation process comes into the rapid growing stage. In this stage, the growing of the oxide is controlled by the diffusion of meltallic cations that form at the oxide/alloy interface via reaction:

$$Mg = Mg^{2+} + 2e^- \tag{4}$$

The lage-scale growth of MgO leads to the depletion of Mg and the richness of the Be under the outer MgO layer. This concentration change of Mg and Be will change the thermodynamic condition, therefore, BeO might form under the outer layer via the reduction reaction:

$$MgO + Be = Mg + BeO \tag{5}$$

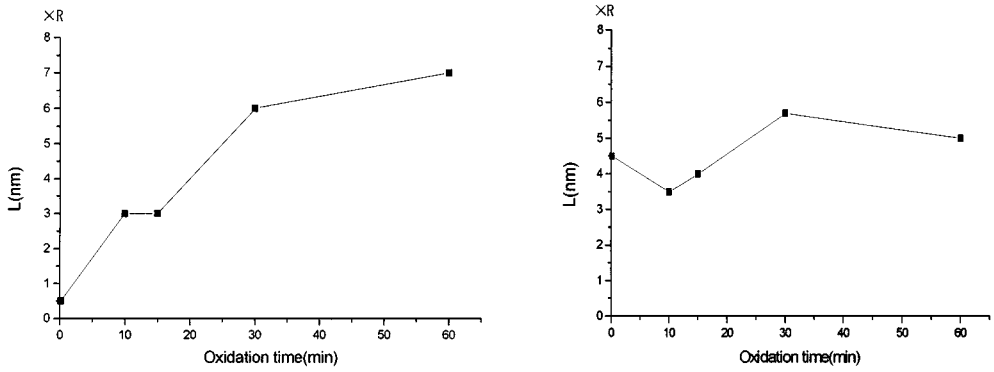


(a)The thickness of the outer layer with time

(b) The thickness of the inner layer with time

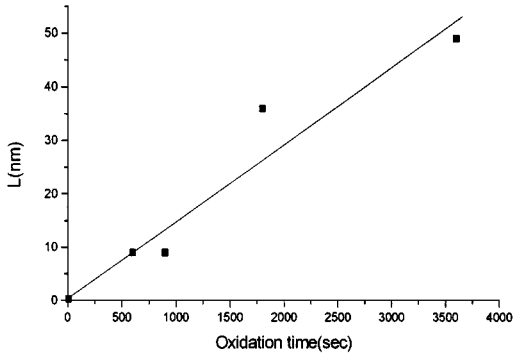


(c)The square of the outer layer thickness with time

*Figure 3* Kinetic curve of the surface oxide film.

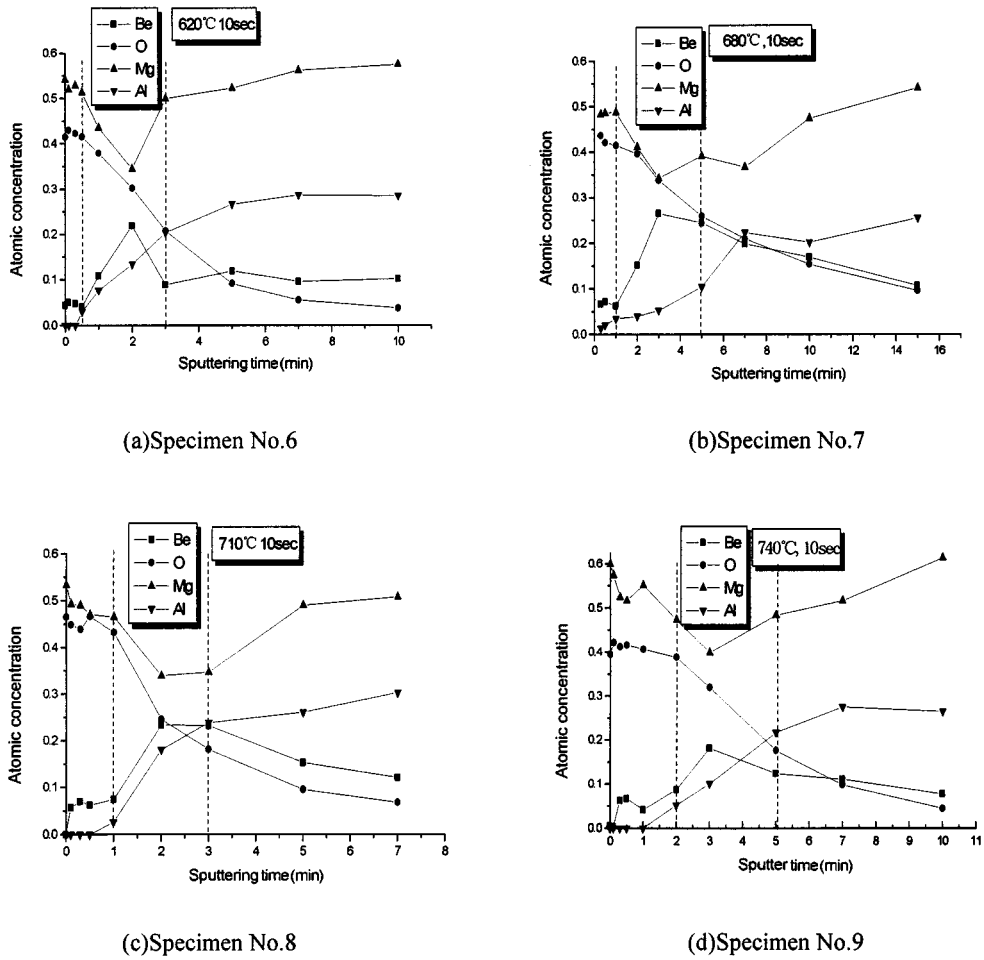


(a)Specimen No.6

(b)Specimen No.7

(c)Specimen No.8

(d)Specimen No.9

*Figure 4* Depth profiles on the surface oxides of specimen No. 6 to 9.

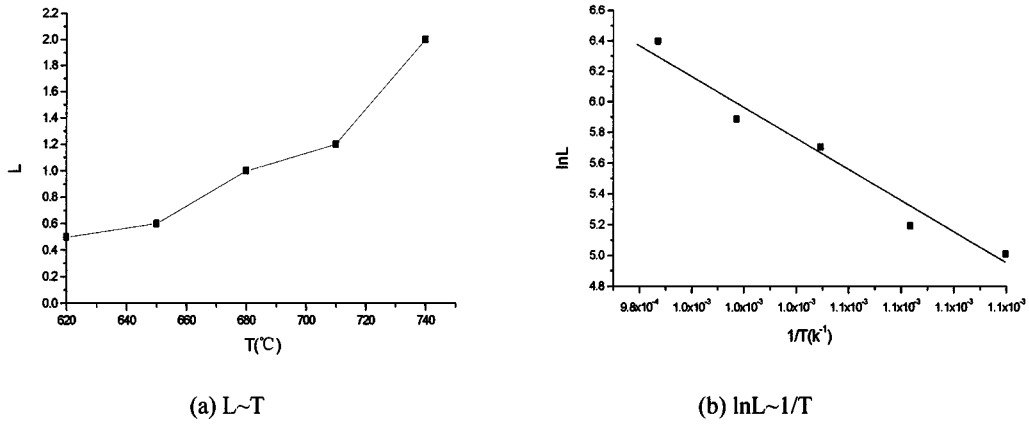


(a) L~T (b) lnL~1/T

*Figure 5* The thickness of the outer layer as the function of the oxidation temperature.

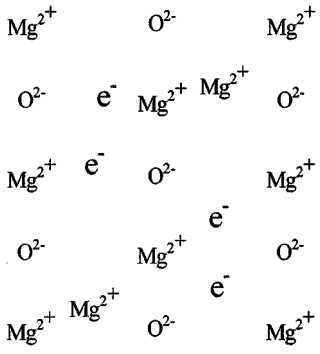


*Figure 6* Interstitial cations and electrons in MgO.

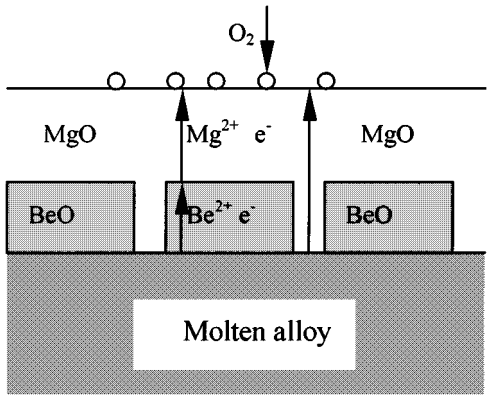


*Figure 7* The oxidation model of the molten Mg-9Al-0.5Zn-0.3Be alloy.

As the result of the reduction reaction, the concentrations of Mg and Be will reach equilibrium at the interface between the outer layer and the inner layer. The oxidation temperature is so high that the above two stage will be finished in quite short time. Within the inner layer, the concentration of the oxidized magnesium decreases and the concentration of the metallic magnesium increases with the depth decreasing.

After the inner layer forms, the oxidation process will come into the steady growing stage. Because BeO has uniform and dense structure, the interstitial $Mg^{2+}$ is hard to diffuse through BeO oxide, so most of them will diffuse through MgO in the inner layer. That is to say, the effective diffusion area under the outer layer is reduced greatly by BeO and the growing rate of the outer layer declines as a result of the sharply decreasing of $Mg^{2+}$ from the inner layer.

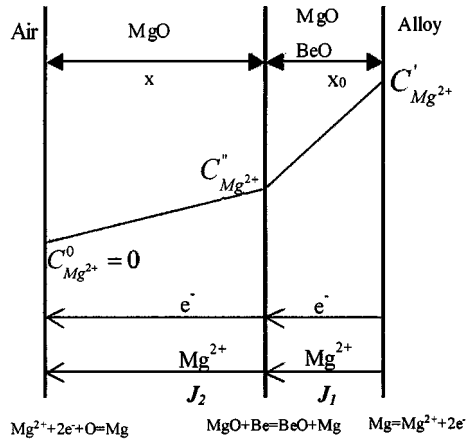


*Figure 8* Diffusion moldel on the surface of the molten.

Fig. 8 is used to perform the kinetic calculation. During the steady growing stage, the concentrations of $Mg^{2+}$ at the outer/inner layer interface and the oxide/alloy interface are believed to be constant. According to the first Fick diffusion law [18], the diffusion flux in the inner layer can be expressed by:

$$J_1 = -D_1 \frac{C'_{Mg^{2+}} - C''_{Mg^{2+}}}{X_0} \tag{6}$$

where $D_1$ is the diffusion coefficient of $Mg^{2+}$ in the inner layer, $C''_{Mg^{2+}}$ and $C'_{Mg^{2+}}$ denote the concentration of interstitial $Mg^{2+}$ at the outer/inner layer and the oxide/alloy interface respectively.

No new MgO forms in the inner layer during the steady growing stage, so it is easy to understand that the inner layer will hardly thicken in the later time. For the outer layer, it thickens continuously because MgO forms on the air/oxide interface continuously. The diffusion flux of the outer layer is expressed by:

$$J_2 = -D_2 \frac{C''_{Mg^{2+}} - C^0_{Mg^{2+}}}{X} \tag{7}$$

where $D_2$ is the diffusion coefficient of the interstitial $Mg^{2+}$ in the outer layer, $C^0_{Mg^{2+}}$ denotes the interstitial $Mg^{2+}$ concentration at the air/oxide interface and is

about to be zero. Thus, the growing rate of the outer layer can be deduced:

$$\frac{dX}{dt} = C_1 J = \frac{-C_1 D_2 C''_{Mg^{2+}}}{X} = \frac{k'}{X} \quad (8)$$

$$k' = -C_1 D_2 C'_{Mg^{2+}} \quad (9)$$

$C_1$ and $k'$ are constant. Integrating both size of the Equation 8, the kinetic equation of the outer layer can be deduced as:

$$X^2 = 2k't = kt \quad (10)$$

$$k = 2k' \quad (11)$$

Equation 10 proves that the inner layer grows under parabolic in theory and is accordant with the experiment result shown in Fig. 4.

Generally, MgO grows under linear law during high temperatures [19]. The growing rate is very high and the structure of MgO film is very loose. While in the present study, the density and tough mixed inner layer decreases the diffusion rate of the outer $Mg^{2+}$. Therefore, the diffusion becomes the controlling factor during oxidation and the outer MgO layer grows under the parablic law.

If the oxidation time $t$ is kept unchanged as $t_0$, then the following equation will be got.

$$X^2(T, t_0) = k(T)t_0 \quad (12)$$

which indicates $X^2$ is proportional to the parablic constant $k$. Using Arrhenium formula, $D_2$ can be represented by:

$$D_2 = D_0 \exp\left(-\frac{Q}{RT}\right) \quad (13)$$

where $Q$ denotes the activation energy and $R$ is constant. Putting Equations 11 and 13 into 12 we get

$$X^2(T, t_0) = -2C_1 C''_{Mg^{2+}} t_0 D_0 \exp\left(-\frac{Q}{RT}\right) = C_2 \exp\left(-\frac{Q}{RT}\right) \quad (14)$$

where

$$C_2 = -2C_1 C''_{Mg^{2+}} t_0 D_0 = \text{Const}$$

Making natural logarithm on both sizes of Equation 14, the following result can be deduced:

$$\ln X(T, t_0) = C_3 \frac{1}{T} \quad (15)$$

where $C_3$ is constant. That is to say, $\ln X$ is proportional to $1/T$ and the outer layer thickness $X$ is exponential to the oxidation temperature $T$, which is accordant with the experimental results shown in Fig. 5.

## 5. Conclusions

According to above discussions, the following conclusions can be obtained:

1. Be promotes the oxidation resistance of magnesium alloy by forming a denser and tougher oxide film on the surface of molten Mg-9Al-0.5Zn-0.3Be magnesium alloy.
2. The oxide film growing on the surface of the molten Mg-9Al-0.5Zn-0.3Be alloy is considered to be dual structure: outer layer (MgO) and inner mixed layer (BeO+MgO).
3. The growth of the outer layer follows parabolic law, but the inner layer grows slowly and linearly.
4. The exponential relationship, which is proved by theory deducing and experimental results, exists between the thickness of the outer layer and the oxidation temperature.


## Acknowledgement

Helpful discusses with Senior Engineer Zhou Huiliang on AES analysis are gratefully acknowledged.


## References


1. D. MAGERS, *Light Metal Age* **55**(7/8) (1997) 60.
2. R. BROWN, *ibid.* **55**(7/8) (1997) 72.
3. B. B. CLOW, *Advanced Materials & Processes* **150**(10) (1996) 33.
4. I. K. HOWARD, *Light Metal Age* **51**(4) (1993) 22.
5. S. C. ERICKSON, J. F. KING and T. MELLERUD, *Foundry Management & Technology*, **126** (6) (1998) 38.
6. J. W. FRUEHLING and J. D. HANAWALT, *AFS. Trans.* **77** (1966) 159.
7. M. MAISS and C. A. M. BRENNINGKMEIJER, *Environments Science and Technology* **20** (1998) 3077.
8. S. L. COULING and F. C. BENNETT, *Light Metal Age* **35**(10) (1977) 12.
9. M. GILBERT, Japanese Patent, 69 623 (1924).
10. R. A. U. HUDDLE, J. LAING, A. C. JESSUP and E. F. EMLEY, UK Patent, 776649 (1953).
11. G. FOERSTER, *Advanced Materials & Processes* **154** (4) (1998) 79.
12. M. SAKAMOTO and S. AKIYAMA, *J. Mater. Sci. Lett.* **16** (1997) 1048.
13. S. AKIYAMA, *Journal of Japan Foundry Engineer Society* (1994) 38.
14. F. L. BRUKETT, *AFS. Trans.* **2** (1954) 442.
15. K. B. WIKLE, *ibid.* **26** (1978) 513.
16. L. E. DAVIS, N. C. MACDONALD, P. W. PALMBERG, G. E. RIACH and R. E. WEBER, in "Handbook of Auger Electron Spectroscopy" (2nd ed). (Physical Electronics Industries Division, Minnesota, 1976).
17. CUI ZHONGYI, "Metallurgy and Heat Treatment" (Chinese) (Mechanical Industry Press, Beijing, 1989) p. 226.
18. ZHAI JINKUN, "High temperature corrosion of Metals" (Chinese) (Beijing University of Aerospace and Aviation Press, Beijing, 1990) p. 50.
19. ZHU RIZHANG, HE YEDONG and QI HUIBIN, "High Temperature Corrosion and High Temperature Anti-Corrosion Materials" (Chinese) (Shanghai Science Technology Press, Shanghai, 1995) p. 131.



*Received 10 May*
*and accepted 13 November 2000*